Biomimetic formation of chicoric-acid-directed luminescent silver nanodendrites

2012 Nanotechnology 23 294011

(http://iopscience.iop.org/0957-4484/23/29/294011)

Nanotechnology **23** (2012) 294011 (9pp) doi:10.1088/0957-4484/23/29/294011

Biomimetic formation of chicoric-acid-directed luminescent silver nanodendrites

Stacey N Barnaby[1,3], Nazmul H Sarker[1], Areti Tsiola[2,4] and Ipsita A Banerjee[1]

[1] Department of Chemistry, Fordham University, 441 East Fordham Road, Bronx, NY 10458, USA
[2] Department of Biology, Queens College, City University of New York, 65-30 Kissena Boulevard, Flushing, NY 11367, USA

E-mail: banerjee@fordham.edu

Received 7 November 2011, in final form 21 February 2012
Published 28 June 2012
Online at stacks.iop.org/Nano/23/294011

Abstract
In this work, we report the formation of well-defined silver nanodendrites via biomineralization under mild conditions in a single step, in the presence of the plant phytohormone chicoric acid (CA), a well-known HIV-I integrase inhibitor. CA played a dual role as reductant as well as directed the growth of the nanodendrites, which were found to grow primarily in the [111] and [200] directions. In addition to the formation of highly ordered hierarchical structures, the formed Ag nanodendrites were found to exhibit luminescence, as observed by confocal microscopy. This study not only demonstrates a new method for the preparation of luminescent silver nanodendrites using a simple, environmentally friendly biological method, but also indicates the ability of CA, a potent HIV-integrase inhibitor, to interact with silver ions which may shed light on its potential for additional biomedical and biosensor applications.

S Online supplementary data available from stacks.iop.org/Nano/23/294011/mmedia

(Some figures may appear in colour only in the online journal)

1. Introduction

The design and fabrication of nanostructures with tunable dimensions has attracted much interest due to their wide range of applications in the development of nanoelectronic devices, sensors, solar cells, biomedical and imaging processes [1–5]. In particular, the design of inorganic nanostructures with shape-controlled morphologies has gained tremendous momentum due to their ensuing effects on the optical, electrical and magnetic properties [6]. Multiple-branched hierarchical nanostructures have been fabricated due to their host of applications in photovoltaics, nanoelectronics and biosensor devices [7, 8]. For example, Y-junction carbon nanotrees, WO_3 nanoforests [9, 10], $FeCl_3$–S [11], GaP, Nb_2O_5, alumina and ZnO/CuO hierarchical nanotrees have been prepared [12–15]. However, in most cases, the synthesis of such organized nanotrees and nanodendritic structures require the use of high temperatures and relatively harsh reaction conditions. Commonly utilized approaches include hydrothermal synthesis, chemical vapor deposition, photolithography-assisted wafer scale fabrication, liquid phase reduction, solvothermal and electrochemical methods [16–19]. However, the preparation of such intricate branched structures via environmentally friendly biomimetic means is relatively less common. Over the past decade, biomimetic methods for the growth of morphology-controlled nanocrystals have been gaining popularity due to the molecular recognition ability of the biomolecules [20]. Efforts have been focused on using viruses, fungi, plants and peptides devised from combinatorial phage libraries as well as various oligonucleotides [21–24]. Recently dendritic gold, silver, palladium and platinum nanostructures with controlled morphologies were synthesized using a variety of mild synthetic methods [25]. For example,

[3] Present address: Department of Chemistry, Northwestern University, 2145 Sheridan Road, Evanston, IL 60208, USA.
[4] Present address: Queensboro Community College, 222–5 56th Avenue, Bayside, NY 11364, USA.

polymers such as poly(vinyl pyrrolidine) (PVP) have been utilized as capping agents as well as a template to facilitate the growth of dendritic structures [26]. $LiFePO_4$ nanodendrites have been synthesized in ethyleneglycol/water in the presence of a sodium dodecyl benzene sulfonic acid surfactant [27]. Additionally, morphology-controlled Pd–Pt bimetallic nanodendrites consisting of an array of Pt branches formed on Pd cores were synthesized using L-ascorbic acid in the presence of Pd nanocrystal seeds under aqueous conditions [28]. In particular, silver dendritic nanostructures have been prepared in the presence of tetrathiafulvalene, ascorbic acid, ethylene diamine tetraacetate or via UV irradiation [29]. Template-free approaches to form Ag dendritic structures using zinc microparticles as a heterogeneous reducing agent have also been utilized [30]. In related work, Ding and co-workers synthesized Ag dendritic structures by replacement reaction in the presence of zinc plates [31]. Such dendritic structures with trunks, hierarchical branches and leaflets have intricate structural characteristics and, therefore, are touted to be highly favored structures for the preparation of advanced nanodevices [32]. It is therefore necessary to devise methods to create such hierarchical structures via simple, economical means for large scale applications.

In this work, we have fabricated highly ordered dendritic Ag nanostructures by mild biomimetic means in the presence of CA, also known as dicaffeoyltartaric acid, a well-known plant phytohormone with several medicinal properties including its utility as a potent HIV-integrase inhibitor [33]. Our method provides a facile single-step approach for preparing complex dendritic silver nanostructures at room temperature by integrating both the chelating and mineralization ability of CA which leads to the formation of supramolecular complexes that direct the formation of Ag nanodendrites. Further, this work may shed light into the metal chelating abilities of a potent biomolecule such as CA.

2. Experimental section

2.1. Materials

Chicoric acid (CA) was purchased from Sigma Aldrich and silver nitrate was purchased from Fisher Scientific. All materials were utilized as received. All solutions were prepared in double-distilled water, purified by a Milli-*Q* system.

2.2. Methods

Formation of the Ag dendrites in the presence of CA: varying concentrations of silver nitrate (0.5–5 mM) were added to an aqueous solution of CA (1 mM) in order to examine its effect on the formation of Ag nanoparticles. $AgNO_3$ (99%) was added drop-wise to an aqueous solution of CA until the desired concentration was reached. The nanoparticles and dendritic structures were allowed to grow at room temperature and the formation of the nanostructures was examined over time by fluorescence excitation and emission spectroscopy. The morphologies of the nanostructures formed were probed by transmission electron microscopy (TEM) and scanning electron microscopy (SEM). The samples were centrifuged and washed twice with double-distilled water before analyses.

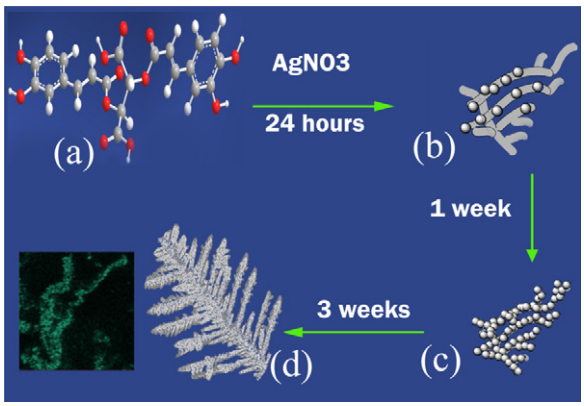

Scheme 1. Biomimetic growth of silver nanodendrites in the presence of chicoric acid over a period of three weeks. (a) Chemical structure of chicoric acid. (b) Growth of Ag nanoparticles on CA assemblies. (c) Formation of branched structures after one week. (c) Ag dendritic structures after three weeks of growth. The inset shows the confocal image of the Ag dendrites.

3. Results and discussion

In general, plant polyphenols are abundantly present in food sources such as berries, herbs and certain vegetables and have excellent antioxidant properties which help in minimizing free radical damage biologically [34]. From a materials standpoint, the presence of the phenolic hydroxyl groups aids in chelating with metal ions and in some cases result in their reduction, forming corresponding metal nanoparticles either by a hydrogen transfer or electron transfer mechanism [35–37]. The chemical structure of CA is shown in scheme 1. As shown, CA contains two phenolic hydroxyl groups in addition to two carboxyl groups. We hypothesized that, due to its characteristic functional groups, CA may potentially serve as a prime molecule to aid in the reduction of silver ions and assist in the directed formation of hierarchical nanostructures. Scheme 1 illustrates the step-by-step process involved in the formation of the dendritic structures. In order to explore the potential of CA to aid in the formation of Ag nanoparticles biomimetically, an aqueous solution of CA was treated with silver nitrate at room temperature. As shown in figure 1, initially spherical Ag nanoparticles are formed. The formation of Ag nanoparticles in the presence of CA most likely occurs due to the two-electron oxidation of the hydroxyl groups of the phenol ring system of CA, leading to the formation of a quinoid-containing keto–enol system as seen in other plant phenols [38]. Further, CA appears to play a dual role: (a) complex with silver ions, followed by nucleation of Ag nanoparticles; and (b) to direct the formation of the hierarchical Ag dendrites by controlling the

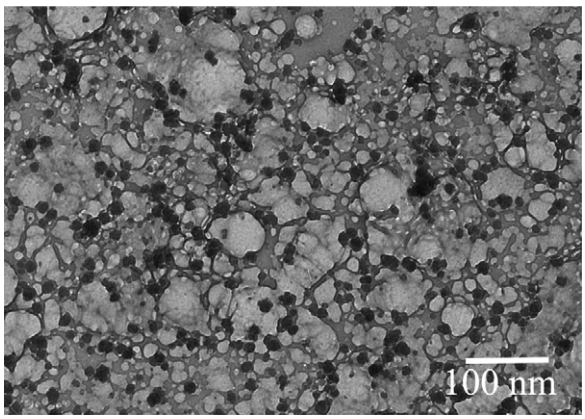

Figure 1. Supramolecular assemblies of spherical Ag nanoparticles bound to CA assemblies after one day of growth.

orientation of specific crystal lattices, as well as corresponding surface energies. In the past, crystal growth in a particular axis has been shown to be controlled by peptides, surfactants or DNA [39]. In the presence of the phytohormone CA, we observed that initially spherical Ag nanoparticles which grow along the surface of the CA assemblies are formed and the interactions with CA promote further reduction of silver ions at the interface between CA and silver ions. The formation of CA networks is attributed to hydrogen-bonding interactions between the carboxyl and hydroxyl groups as well as coordination with silver ions. The formation of such fibrillar networks of biomolecules in the presence of metal ions have been reported in chemically modified single-stranded DNA, which displayed altered structures upon binding to metal ions (Zn^{2+} or Fe^{2+}) [40]. Additionally, several peptide sequences have shown unique conformational changes upon binding with metal ions. For example, addition of Zn^{2+} ions or Cu^{2+} ions have been shown to modulate the assembly kinetics of various segments of beta-amyloid peptides [41, 42]. Plant-based polyphenolic molecules such as theaflavin have also been found to self-associate and complex with caffeine forming dimers by stacking interactions [43].

The proposed multi-step mechanism involved in the formation of the dendrites is explained as follows. The first step involves the coordination of the Ag^{+} ions with the hydroxyl and carboxyl groups of CA followed by reduction of the ions, leading to the formation of the initial spherical silver nanoparticles on the formed CA assemblies. A proposed model showing the binding of the Ag ions to CA molecules is shown in (figure 2), indicating each layer of CA is coordinated via the carboxyl groups as well as –OH groups, leading to the formation of supramolecular complexes of CA with silver ions. The Ag^{+} ions continue to diffuse into the CA assemblies and are reduced to form silver nanoparticles. As the growth continues, the nanocrystals continue to come together and grow in size, due to nucleation and growth on preformed silver nanocrystals (figures 3(a) and (b)), which results in the lowering of surface energy. Interfaces between the nanocrystals are seen (figure 3(c)) which over time disappear and eventually develop into the trunk of the dendritic nanostructures (figure 3(d)). As the nanocrystals are continuously reduced, they attach to the sides of the trunk and continue to grow in size, forming anisotropic nanocrystals showing a blend of fractal and dendritic character along with smaller aggregates which tend to attach to the tips leading to the formation of the branches and leaves (figure 3(e)).

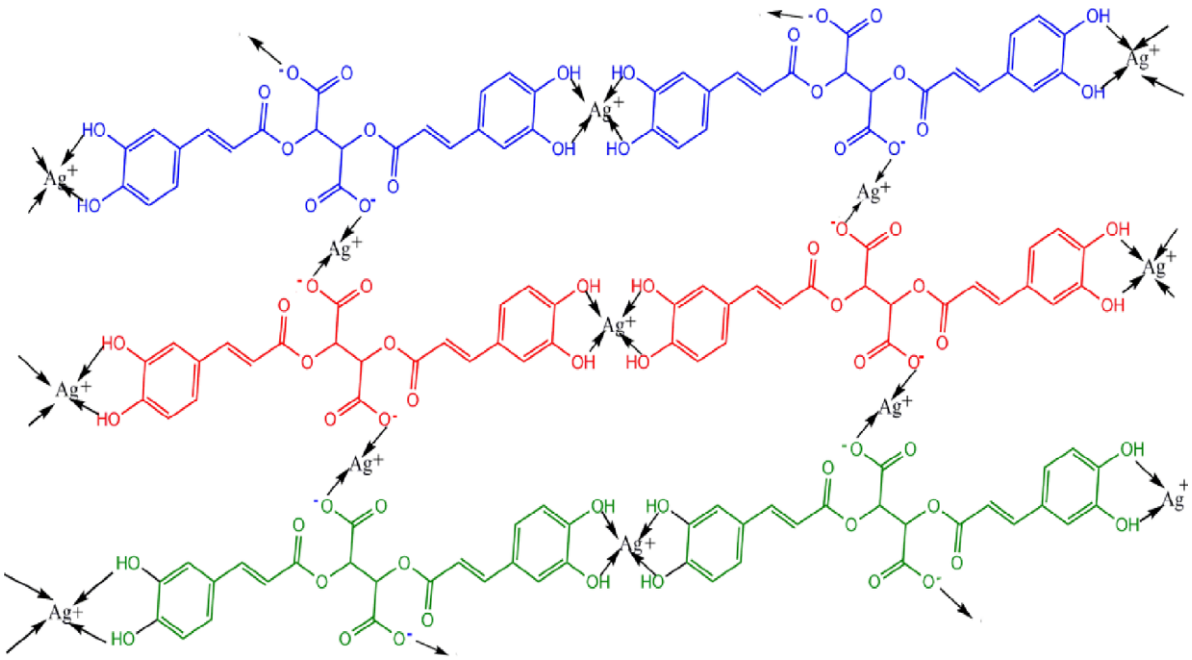

Figure 2. Proposed mechanism for the coordination of silver ions with CA. Three different layers are shown (represented in blue, green and red).

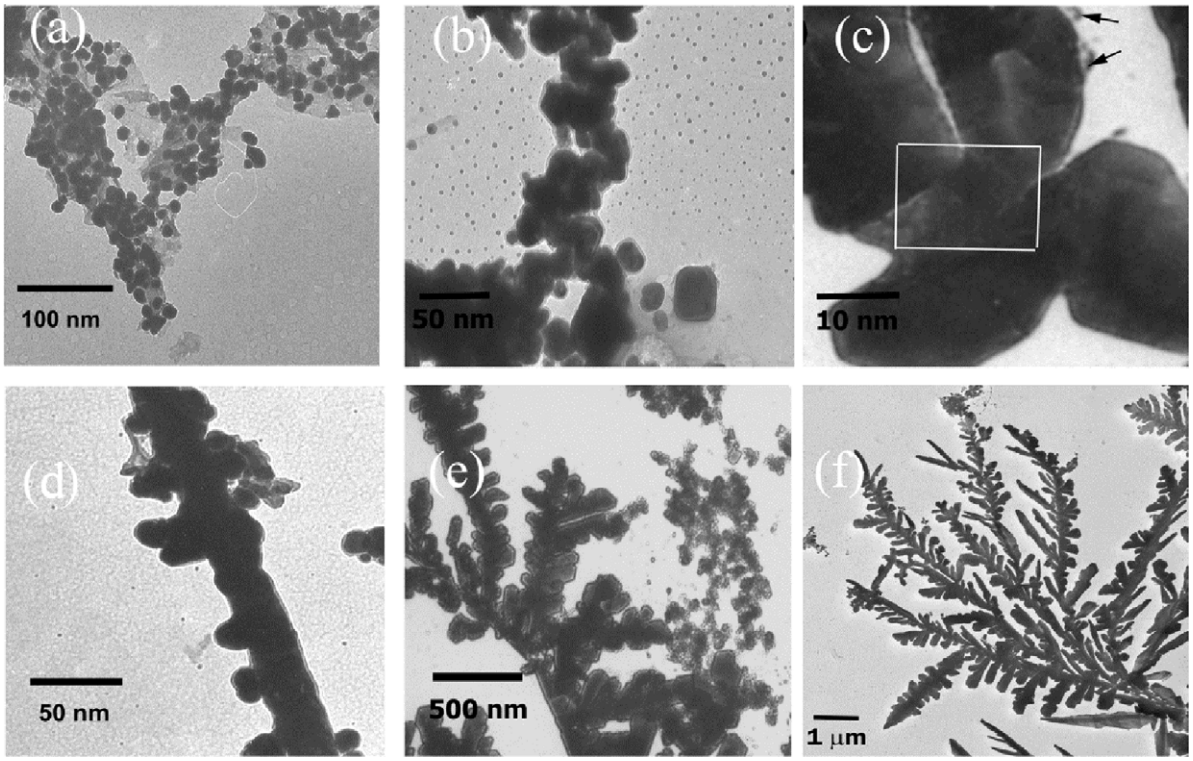

Figure 3. Growth of silver nanodendrites over time. (a) Growth after two days showing spherical nanoparticles on CA assemblies. (b) Growth after 4–5 days showing the nanoparticles coming together. (c) Integration of the nanoparticles. The area within the square shows the interfaces formed between the nanoparticles; the arrows indicate edge defects. (d) Growth after one week showing the trunk and formation of branches. (e) After 10–12 days showing the growth of leaves and branches. (f) Ag dendrites formed after 17 days.

Ultimately hierarchical dendritic structures are formed over a period of three weeks (figure 3(f)). It is well known that growth rates of anisotropic nanocrystals are dependent on the surface energies of the crystallographic planes [44]. In our case, hexagonal silver nanocrystals forming the leaves continue to grow on the preformed silver nuclei, leading to the preferential crystal growth along [111] and [200] directions as shown in the SAED (figure 4(a)). The formation of the dendritic nanocrystal structures appears to be due to the lower surface energy along the [111] and [200] crystal growth axes. Figure 4(b) shows the HRTEM image of the Ag nanoleaves and the lattice fringes were measured to be 0.204 nm, which is in agreement with the {111} lattice spacing of the fcc crystal. Edge dislocations formed at the assembling interfaces are also observed (figure S1, supplementary data available at stacks.iop.org/Nano/23/294011/mmedia) and allow for specific oriented attachment [45]. In addition to dislocations, defects such as twining and stacking are observed in the nanocrystals forming the hierarchical structures where the hexagonal leaflets gradually form long fern leaflet structures (figure S2, supplementary data available at stacks.iop.org/Nano/23/294011/mmedia). As the process continues, over time (four weeks) intricate fern-like structures are observed as shown in figure 5 and figure (S3, supplementary data available at stacks.iop.org/Nano/23/294011/mmedia). Thus, large dendritic hyper-branched microstructures are ultimately formed over longer periods of time (figure 6) partly due to overlap of the branches and aggregation behavior. In general,

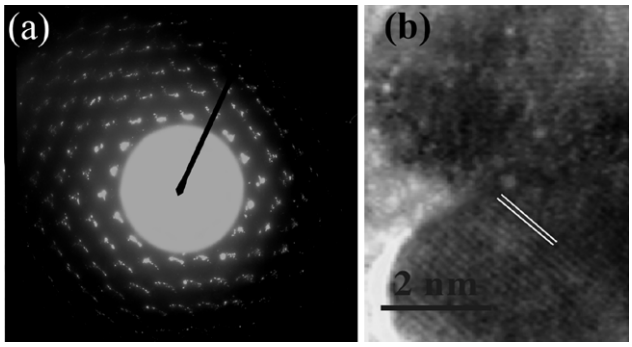

Figure 4. SAED pattern showing the growth of the hexagonal nanocrystals in [111] and [200] directions. (b) HRTEM image of Ag nanoleaves in the [111] and [200] directions. $d = 0.204$ nm.

the growth was found to be dependent on the concentration of silver ions as well as CA, where the optimum ratio was found to be a 1:2 ratio of CA to Ag ions. At lower concentrations, the formation of dendrites was not observed, while at very high concentrations, mostly aggregates were observed (figure S4, supplementary data available at stacks.iop.org/Nano/23/294011/mmedia). The optimum concentration of silver ions was found to be in the range of 1.5–2 mM.

FTIR spectroscopy (figure 7) was employed in order to confirm the binding interactions of CA with Ag ions. The spectrum of the CA monomer shows C=O stretching

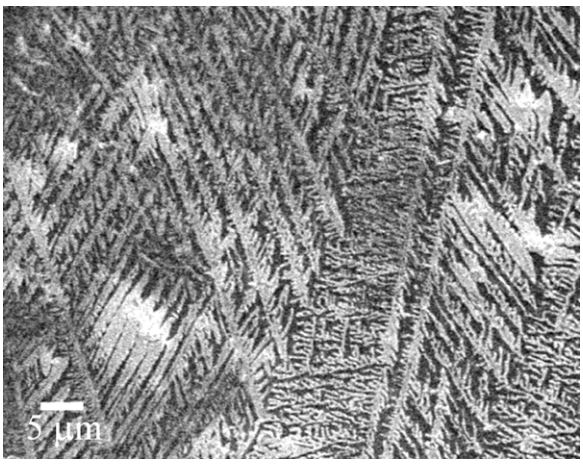

Figure 5. Formation of Ag microferns after four weeks of growth.

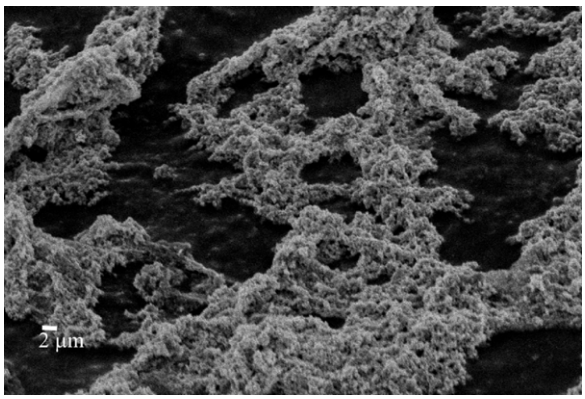

Figure 6. SEM image showing multiple hyper-branched Ag micro-dendrite structures, after three months of growth.

peaks at 1724 and 1697 cm^{-1}, with a split at 1653 cm^{-1}. These peaks are assigned to hydrogen-bonded C=O peaks and non-hydrogen-bonded peaks, respectively. The formation of the Ag dendrites causes a shift, to 1704 and 1690 cm^{-1}, with a short shoulder at 1652 cm^{-1}, due to disruption in hydrogen-bonding interactions compared to the monomer. This indicates that the carboxyl group is involved in coordination with the silver ions. In previous work, a similar splitting of the carboxyl band was observed when bromoisobutyric acid (BPA) complexes with ZnO were formed due to bridging of the carboxylate bidentate ligands [46]. An additional peak at 1557 cm^{-1} is observed which is assigned to quinoid stretching vibration [47]. In the case of the CA monomer, a broad hydroxyl peak was seen at 3474 cm^{-1}, while upon formation of Ag dendritic structures the peak was significantly diminished and shifted to 3465 cm^{-1}, which is indicative that the hydroxyl groups are also involved in coordination with Ag ions. Similar results have been reported in other work, where it has been shown that, upon complexation of catechol with metal oxides, there was a decrease in the –OH peak intensity, indicating that complexation occurs with the phenolic groups [48].

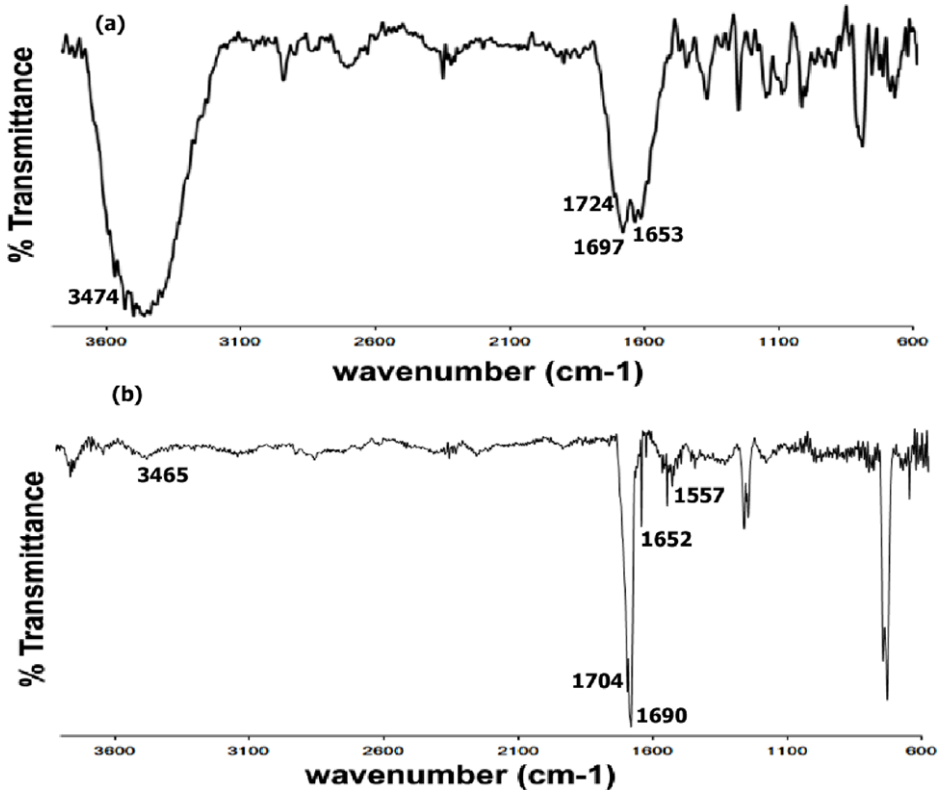

Figure 7. Comparison of FTIR spectra of (a) CA and (b) Ag nanodendrites formed in the presence CA.

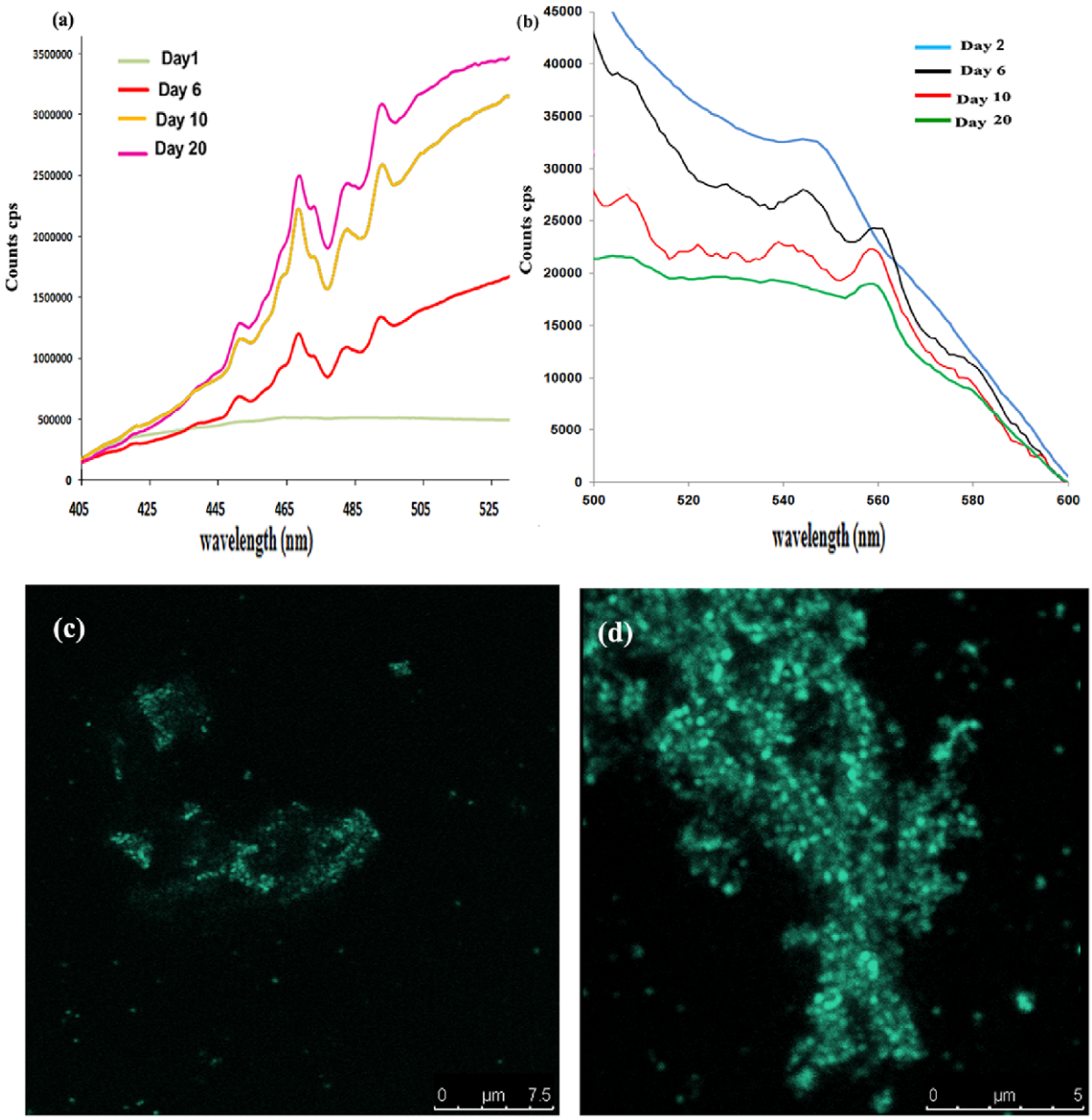

Figure 8. Excitation (a) and emission (b) spectra at different periods of growth of Ag nanodendrites. (c) Fluorescence confocal microscopy image after five days. (d) Fluorescence confocal microscopy image after three weeks of growth.

Silver nanoparticles are often utilized as nanomarkers in imaging [49a]. For example, Ag nanoparticles have been utilized in stabilizing the fluorescence signal of organic fluorophores by suppressing Cy5 photoinduced blinking and photobleaching [49b]. In another study, luminescent silver dendritic structures were used for the separation and detection of DNA [50]. To determine the luminescence properties of the formed silver dendritic structures, we conducted spectroscopic analyses. As shown in figure 8(a), the excitation spectra initially show a short peak at 410 nm. Over time a redshift and additional peaks at 450, 481 and 492 nm were observed as the growth of the dendrites progressed due to excitation of localized surface plasmon resonances (LSPR). Similar redshifts were also observed in the UV–vis spectra (figure S5, supplementary data available at stacks.iop.org/Nano/23/294011/mmedia) due to LSPR [51]. This observation is in accordance with the Mie theory [52]. In general, for larger metal nanoparticles, the plasmon resonances depend mainly on their sizes and higher-order modes become more significant as the sizes of the particles grow. As shown in the absorption and excitation spectra, these higher-order modes peak at lower energies [53] and thus the plasmon band redshifts with increasing particle size.

The fluorescence spectra initially (figure 8(b)) show a lambda max at 560 nm. As the growth progressed there was a gradual decrease in the intensity at 560 nm and the appearance of a new peak at 570 nm due to the formation of the dendritic structures was observed. Confocal microscopy conducted shows that the silver dendrites were luminescent. Figure 8(c) shows the fluorescence confocal image obtained after five

days of growth, showing the Ag nanoparticles coming together, while figure 8(d) (after three weeks of growth) shows the structure of an entire nanodendritic structure exhibiting luminescence.

4. Conclusions

In summary, dendritic structures of silver were formed biomimetically in the presence of the plant phytohormone CA in a single step. We believe that examining the interactions of CA with metal ions may shed light into the mechanistic implications involved in the metal ion binding properties of the biomolecule. CA played a vital role in promoting the growth of the hierarchical nanostructures by reducing silver ions as well as controlling the growth of the structures along the [111] and [200] crystal axes. The luminescent Ag dendrites illustrate the possibility of incorporating functional elements for photonics applications as well as for imaging, sensors or SERS applications. Such control of morphology suggests the tremendous potential for utilization in nanoscale devices and systems. In addition, such luminescent ordered nanostructures can be potentially integrated within microfluidic channels and applied in high-throughput biosensors.

Acknowledgments

This work was conducted in part using equipment from the Queens College Facilities for Imaging, Cell and Molecular Biology. The financial support provided by the Dean's Office Fordham University Faculty Research Grant is acknowledged (IB). SB and NS thank the Fordham University Summer Science Internship program for financial support.

References

[1] Aguirre C M, Ternon C, Paillet M, Desjardins P and Martel R 2009 Carbon nanotubes as injection electrodes for organic thin film transistors *Nano Lett.* **9** 1457–61
Giljohann D A, Seferos D S, Massich M D, Daniel W L, Patel P C and Mirkin C A 2010 Gold nanoparticles for biology and medicine *Angew. Chem.* **49** 3280–94

[2] Hasobe T, Fukuzumi S and Kamat P V 2006 Organized assemblies of single wall carbon nanotubes and porphyrin for photochemical solar cells: charge injection from excited porphyrin into single-walled carbon nanotubes *J. Phys. Chem.* B **110** 25477–4584

[3] Liong M, Lu J, Kovochich M, Xia T, Ruehm S G, Nel A E, Tamanoi F and Zink J I 2008 Multifunctional inorganic nanoparticles for imaging, targeting and drug delivery *ACS Nano* **2** 889–96

[4] Otte M A, Sepúlveda B, Ni W, Juste J P, Liz-Marzán L and Lechuga L M 2010 Identification of the optimal spectral region for plasmonic and nanoplasmonic sensing *ACS Nano* **4** 349–57

[5] Stampfer C, Jungen A, Linderman R, Obergfell D, Roth S and Hierold C 2006 Nano-electrochemical displacement sensing based on single-walled carbon nanotubes *Nano Lett.* **6** 1449–53

[6] Lu L T, Tung L D, Robinson I, Ung D, Tan B, Long J, Copper A I, Farnig D G and Thanh N T K 2008 Size and shape controlled water soluble magnetic cobalt nanoparticles using polymer ligands *J. Mater. Chem.* **18** 2453–8
Teranishi T, Kurita R and Shape M M 2000 Control of Pt nanoparticles *J. Inorg. Organomet. Polym.* **10** 145–56
Nandwana V, Elkins K E, Poudyal N, Chaubey G S, Yano K and Liu J P 2007 Size and shape control of FePt nanoparticles *J. Phys. Chem.* C **111** 4185–9
Scher E C, Manna L and Alivisatos A P 2003 Shape control and applications of nanocrystals *Phil. Trans. R. Soc.* A **361** 241–57

[7] Milliron D J, Hughes S M, Cui Y, Manna L, Li J, Wang L W and Alivisatos A P 2004 Colloidal nanocrystal heterostructures with linear and branched topology *Nature* **430** 190–5
Hu J, Bando Y, Zhan J, Yuan X, Sekiguchi T and Goldberg D 2005 Self-assembly of SiO_2 nanowires and Si microwires into hierarchical heterostructures on a large scale *Adv. Mater.* **17** 971–5
Meng G, Jung Y J, Cao A, Vajtai R and Ajayan P M 2005 Controlled fabrication of hierarchically branched nanopores, nanotubes and nanowires *Proc. Natl Acad. Sci. USA* **102** 7074–8
Risveden K, Dick K A, Rydberg P, Samuelson L and Danielsson B 2010 Branched nanotrees with immobilized acetylcholine esterase for biosensor applications *Nanotechnology* **21** 055102

[8] Liu J W, Wang X, Zheng W T, Li J X, Guan Q F, Su Y D, Qi J L and Jiang Q 2007 Alignment of amorphous carbon nanotubes with graphitized branches grown by radio frequency plasma-enhanced chemical vapor deposition *Carbon* **45** 681–4
Sun S, Meng G, Zhang G, Masse J P and Zhang L 2007 Controlled growth of SnO_2 hierarchical nanostructures by a multistep thermal vapor deposition process *Chem.—Eur. J.* **13** 9087–92
Li H B, Wu R, Li J, Sun Y F, Zheng Y F and Jian J K 2011 Growth of AlN nanobelts, nanorings and branched structures *J. Alloys Compounds* **509** 2111–5

[9] Yao Z, Zhu X, Li X and Xie Y 2007 Synthesis of novel Y-junction hollow carbon nanotrees *Carbon* **45** 1566–70

[10] Shibuya M and Miyauchi M 2009 Efficient electrochemical reaction in hexagonal WO_3 forests with a hierarchical nanostructure *Chem. Phys. Lett.* **473** 126–30

[11] Zheng J, Song J, Zhao J, Li L and Zhu Z 2008 Self-assembly of $FeCl_3$–S nanotrees and their application in directed growth of nanofibers *Mater. Lett.* **62** 4069–71

[12] Dick K A, Deppert K, Larsson M W, Mårtensson T, Seifert W, Wallenberg L R and Samuelson L 2004 Synthesis of branched 'nanotrees' by controlled seeding of multiple branching events *Nature Mater.* **3** 380–4

[13] Liu F and Xue D 2010 Fabrication of Nb_2O_5 nanotrees with controlled branching degrees *Phys. Scr.* T **139** 014074

[14] Zhou J, Deng S Z, Chen J, She J C and Xu N S 2002 Synthesis of crystalline alumina nanowires and nanotrees *Chem. Phys. Lett.* **365** 505–8

[15] Dick K A, Deppert K, Martensson T, Seifert W and Samuelson L 2004 Growth of GaP nanotree structures by sequential seeding *J. Cryst. Growth* **272** 131–7
Guo Z, Chen X, Li J, Liu J-H and Huang X-J 2011 ZnO/CuO hetero-hierarchical nanotrees array: hydrothermal preparation and self-cleaning properties *Langmuir* **27** 6193–200

[16] Yao W-T, Yu S-H, Liu S-J, Chen J-P, Liu X-M and Li F-Q 2006 Architectural control syntheses of CdS and CdSe nanoflowers, branched nanowires and nanotrees via a Solvo thermal approach in a mixed solution and their photocatalytic property *J. Phys. Chem.* B **110** 11704–10

[17] Cheng C, Yan B, Wong S M, Li X, Zhou W, Yu T, Shen Z, Yu H and Fan H J 2010 Fabrication and SERS

performance of silver-nanoparticle decorated Si/ZnO nanotrees in ordered arrays *ACS Appl. Mater. Interfaces* **2** 1824–8

[18] Kawasaki J K and Arnold C B 2011 Synthesis of platinum dendrites and nanowires via directed electrochemical nanowire assembly *Nano Lett.* **11** 781–5
Jung Y J, Wei B, Nugent J and Ajayan P M 2001 Controlling growth of carbon microtrees *Carbon* **39** 2195–201

[19] Kai D, Zhu G, Lu L and Graham D 2011 Easy and large scale synthesis of silver nano dendrites: highly effective filler for isotropic conductive adhesives *J. Mater. Eng. Perform.* **21** 353–7

[20] Huang Y, Chiang C-Y, Lee S K, Gao Y, Hu E L, De Yo-reo J and BelcherA M 2005 Programmable assembly of nano architectures using genetically engineered viruses *Nano Lett.* **5** 1429–34
Bali R and Harris A T 2010 Biogenic synthesis of Au nanoparticles using vascular plants *Ind. Eng. Chem. Res.* **49** 12762–72

[21] Gardea-Torresday J L, Gomez E, Peralta-Videa J R, Parsons J G, Troiani H and Jose-Yacaman M 2003 Alfalfa sprouts: a natural source for the synthesis of silver nanoparticles *Langmuir* **19** 1357–61
Mouxing F, Qingbiao L, Daohua S, Yinghua L, Ning H, Xu D, Huixuan W and Jiale H 2006 Rapid preparation process of silver nanoparticles by bioreduction their characterizations *Chin. J. Chem. Eng.* **14** 114–7

[22] Feldheim D L and Eaton B E 2007 Selection of biomolecules capable of mediating the formation of nanocrystals *ACS Nano* **1** 154–9

[23] Nam K T, Lee Y J, Krauland E M, Kottman S T and Belcher A M 2008 Peptide mediated reduction of silver ions on engineering biological scaffolds *ACS Nano* **2** 1480–6

[24] Sarikaya M 1999 Biomimetics: materials fabrication through biology *Proc. Natl Acad. Sci. USA* **96** 14183–5
Mukherjee P *et al* 2001 Fungus mediated synthesis of silver nanoparticles and their immobilization in mycelial matrix: a novel biological approach to nanoparticle synthesis *Nano Lett.* **1** 515–9
Naik R R, Stringer S J, Agarwal G, Jones S and Stone M O 2002 Biomimetic synthesis and patterning of silver nanoparticles *Nature Mater.* **1** 169–72

[25] Yang L, Sun B, Meng F, Zhang M, Chen X, Li M and Liu 2009 One-step synthesis of UV-induced Pt nanotrees on the surface of DNA network *J. Mater. Res. Bull.* **44** 1270–4
Wen X, Xie Y-T, Cheung Mak M W, Cheung K Y, Li X-Y, Rennenberg R and Yang S 2006 Dendritic nanostructures of silver: facile synthesis, structural characterizations and sensing applications *Langmuir* **22** 4836–42
Song Y, Yang Y, Medforth C J, Pereir E, Singh A K, Xu H, Jiang Y, Brinker J, van Swol F and Shelnutt J A 2004 Controlled synthesis of 2-D and 3-D dendritic platinum nanostructures *J. Am. Chem. Soc.* **126** 635–45
Huang T, Meng F and Qi L 2010 Controlled synthesis of dendritic gold nanostructures assisted by supramolecular complexes of surfactant with cyclodextrin *Langmuir* **26** 7582–9
Fan F-R, Attia A, Sur U K, Chen J-B, Xie Z-X, Li J-F, Ren B and Tian Z-Q 2009 An effective strategy for room-temperature synthesis of single-crystalline palladium nanocubes and nanodendrites in aqueous solution *Cryst. Growth Des.* **9** 2335–40

[26] Wei G, Nan C-W, Deng Y and Lin Y-H 2003 Self-organized synthesis of silver chainlike and dendritic nanostructures via a solvothermal method *Chem. Mater.* **15** 4436–41

[27] Teng F, Santhanagopalan S, Asthana A, Geng X, Mho S-I, Shahbazian-Yassar R and Meng D D 2010 Self-assembly of $LiFePO_4$ nanodendrites in a novel system of ethylene glycol-water *J. Cryst. Growth* **312** 3493–502

[28] Lim R, Jiang M, Camargo P H C, Cho E C, Tao J, Lu X, Zhu Y and Xia Y 2009 Pd–Pt bimetallic nano dendrites with high activity for oxygen reduction *Science* **324** 1302–5

[29] Wang X, Naka K, Itoh H, Park S and Chujo Y 2002 Synthesis of silver dendritic nanostructures protected by tetrathiafulavlene *Chem. Commun.* 1300–1
Xiao J, Xie Y, Tang R, Chen M and Tian X B 2001 Novel ultrasonically assisted template synthesis of palladium and silver dendritic nanostructures *Adv. Mater.* **13** 1887–91
Imai H, Nakamura H and Fukuyo T 2005 Anisotropic growth of silver crystals with ethylenediamine tetraacetate and formation of planar and stacked wires *Cryst. Growth Des.* **5** 1073–7
Zhou Y, Yu S H, Wang C Y, Li X G, Zhu Y R and Chen Z Y 1999 A novel ultraviolet irradiation photoreduction technique for the preparation of single-crystal Ag nanorods and Ag dendrites *Adv. Mater.* **11** 850–2

[30] Wen X, Xie Y-T, Cheung Mak M W, Cheung K Y, Li X-Y, Renneberg R and Yang S 2006 Dendritic nanostructures of silver: facile synthesis, structural characterizations, and sensing applications *Langmuir* **22** 4836–42

[31] Fang J X, You H J, Kong P, Yi Y, Song X P and Ding B 2007 Dendritic silver nanostructure growth and evolution in replacement reaction *Cryst. Growth Des.* **7** 864–7

[32] Cölfen H and Mann S 2003 Higher-order organization by mesoscale self-assembly and transformation of hybrid nanostructures *Angew. Chem. Int. Edn* **42** 2350–65
Wang D and Lieber C M 2003 Inorganic materials: nanocrystals branchout *Nature Mater.* **2** 355–6

[33] Lin Z *et al* 1999 Chicoric acid analogues as HIV-integrase inhibitors *J. Med. Chem.* **42** 1401–14
Robinson W E 1998 L-chicoric acid, an inhibitor of human immunodeficiency virus type 1 (HIV-1) integrase improves on the *in vitro* anti-HIV-1 effect of Zidovudine lus a protease inhibitor (AG1350) *Antiviral Res.* **39** 101–11

[34] Kähkönen M P, Hopia A I, Vuorela H J, Rauha J-P, Pihlaja K, Kujala T S and Heinonen M 1999 Antioxidant activity of plant extracts containing phenolic compounds *J. Agric. Food Chem.* **47** 3954–62

[35] Hider R C, Liu Z D and Khodr H H 2001 Metal chelation of polyphenols *Methods Enzymol.* **335** 190–203
McDonald M, Mila I and Scalbert A 1996 Precipitation of metal ions by plant polyphenols: optimal conditions and origin of precipitation *J. Agric. Food Chem.* **44** 599–606
Fazary A E, Taha M and Ju Y-H 2009 Iron complexation studies of gallic acid *J. Chem. Eng. Data* **54** 35–42

[36] Yoosaf K, Ipe B I, Suresh C H and Thomas G K 2007 *In situ* synthesis of metal nanoparticles and selective naked eye detection of lead ions from aqueous media *J. Phys. Chem.* C **111** 12839–47

[37] Leopoldini M, Marino T, Russo N and Toscano M 2004 Anti oxidant properties of phenolic compounds: H-atom versus electron transfer mechanism *J. Phys. Chem.* A **108** 4916–22

[38] Jacob J A, Mahal H S, Biswas N, Mukherjee T and Kapoor S 2008 Role of phenol derivatives in the formation of silver nanoparticles *Langmuir* **24** 528–33

[39] Brown S, Sarikaya M and Johnson E 2000 A genetic analysis of crystal growth *J. Mol. Biol.* **299** 725–32
Lofton C and Sigmund W 2005 Mechanisms controlling crystal habits of gold and silver colloids *Adv. Funct. Mater.* **15** 1197–208

[40] Göritz M and Krämer R 2005 Allosteric control of oligo nucleotide hybridization of metal induced cyclization *J. Am. Chem. Soc.* **127** 18016–7

[41] Licini G and Scrimin P 2003 Metal-ion binding peptides: from catalysis to protein tagging *Angew. Chem. Int. Edn* **42** 4572–5

[42] Dong J *et al* 2007 Engineering metal ion coordination to regulate amyloid fibril assembly and toxicity *Proc. Natl Acad. Sci. USA* **104** 13313–8
Miura T, Suzuki K, Kohata N and Takeuchi H 2000 Metal binding modes of Alzheimer's amyloid β-peptide in insoluble aggregates and soluble complexes *Biochemistry* **39** 7024–31

[43] Charlton A J, Davis A L, Jones D P, Lewis J R, Davies A P, Haslam E and Williamson M P 2000 The self-association of the black tea polyphenol the aflavin and its complexation with caffeine *J. Chem. Soc. Perkin Trans.* 2 **29** 317–22

[44] Tao A R, Habas S and Yang P 2008 Shape control of colloidal metal nanocrystals *Small* **4** 310–25

[45] Penn R L and Banfield J F 1998 Imperfect oriented attachment: dislocation generation in defect-free nanocrystals *Science* **281** 969–71

[46] Kotal A, Paira T K, Banerjee S and Mandal T K 2010 Ultrasound-induced *in situ* formation of coordination organo gels from isobutyric acids and zinc oxide nanoparticle *Langmuir* **26** 6576–82

[47] Nakayama M, Saeki S and Ogura K 1999 observation of electrochemical formation and degradation processes of polyaniline by Fourier-transform infrared spectroscopy *Anal. Sci. Japan. Soc. Anal. Chem.* **15** 259–63

[48] Gulley-Stahl H, Hogan P A, Schmidt W L, Wall S J, Buhrlage A and Bullen H A 2010 Surface complexation of catechol to metal oxides: an ATR-FTIR, adsorption and dissolution study *Environ. Sci. Technol.* **44** 4116–21

[49a] Aslan K, Lakowicz J R and Geddes C D 2005 Metal-enhanced fluorescence using anisotropic silver nanostructures: critical progress to date *Anal. Bioanal. Chem.* **382** 926–33

[49b] Fu Y, Zhang J and Lakowicz J R 2008 Reduced blinking and long-lasting fluorescence of single fluorophores coupling to silver nanoparticles *Langmuir* **24** 3429–33

[50] Yang X, Sun X, Lv Z, Guo W, Du Y and Wang E 2010 Ultra sensitive nucleic acid detection using confocal laser scanning microscope with high crystalline silver dendrites *Chem. Commun.* **46** 8818–20

[51] Haes A J, Zou S, Schtaz G C and Van Duyne R P 2004 A nano scale optical biosensor: the long range distance dependence of the localized surface plasmon resonance of noble metal nanoparticles *J. Phys. Chem.* B **108** 109–16
Kelly K L, Coronado E, Zhao L L and Schatz G C 2003 The influence of size, shape and dielectric environment *J. Phys. Chem. B.* **107** 668–77

[52] Mie G 1908 Contributions to the optics of turbid media, particularly of colloidal metal solutions *Ann. Phys.* **25** 377–445

[53] Bohrén C F and Huffman D R 1983 *Absorption and Scattering of Light by Small Particles* (New York: Wiley)
Kerker M 1969 *The Scattering of Light and Other Electromagnetic Radiation* (New York: Academic)